Variances in Quantum Electronic Characteristics: The Effects of Differing Li, Be, and Na Electrodes with Constant Scattering Regions

Grant Wilkins*

Dobyns-Bennett High School

E-mail: grant.wilkins371@gmail.com

Abstract

Molecular electronics will soon be pervasive in the world of technology. To properly understand the divergence from classical concepts, studies must be conducted to further understand the nature of simple systems at the quantum level. In this exploration, electrodes of differing composition in one atom thick terminals were tested against certain scattering regions to determine device behavior. Through this analysis, new device behavior and understanding was found in the I-V characteristics of Li, Be, and Na electrodes using computational modeling systems such as SIESTA, tranSIESTA, and NWChem. With the Li and Na electrodes acting similarly to transistors and the Be electrodes having a recurring diode-like behavior, new behaviors that should be further studied have been discovered.

Introduction

In recent years, the trend of technological development has shown simultaneously increasing computational power and decreasing physical size.[1] By reducing dimensions, not only does one increase compartmentalization, but the efficiency of the circuitry and devices is also increased, allowing less power dissipation and broader device capability. A case that exemplifies the tendency for reducing a device's size is the well-documented Moore's law, which notes that the number of transistors in a circuit doubles every two years, a feat that can only occur with shrinking wiring and switches.[2] However, as the circuitry shrinks, the density of atoms and generalized operation of the device change as well. At a certain size, the ability to ignore the atomic effects described by quantum mechanics is diminished and this behavior must become the focal point of design and behavior modeling for these minute devices.[3] In this study, these quantum effects will be viewed through the lens of variations upon a nanoscale electrode and wiring system, allowing the possibilities for future development in devices to be expanded and more deeply understood.

At the scale of inspection, quantum effects contribute to a wide array of non-classical behavior in how atoms act electronically. In a classical wiring system, measured charges flow through a path as determined by the wire. Because the system is macroscopic to the point of ignoring quantum effects, experimental extrapolations such as Ohm's Law can accurately describe the system. Yet when a wire is only a single or a few atoms thick, electron transport behaves differently leading to less simple characteristics.

One effect largely responsible for this behavior is quantum tunneling.[4] This transport phenomenon is a result of the probabilistic interpretation of a particle's location as completely described by the wave-function $\mathbf{\Psi}(\mathbf{x}, t)$.[5] This effect is intrinsically non-classical because electrons are not bound to the macro-wire path, allowing a non-uniform current behavior.

Tunneling also applies to the situation of molecular wiring and affects the modeling of nanoscale devices and how an applied voltage changes the battery's operations. In this case, approximations of the Kohn-Sham wave functions are necessary to determine information

about the system.[6] For many-particle systems this leads to non-homogenous forms that require large scale reductions and methods, meaning computational systems should be utilized to increase accuracy.[7,8]

For this task, the method density functional theory (DFT) is used to approximate the energy and hence can be tasked to compute other results from the given system.[9] Energy exchange and correlation interactions occur using first principles as an *ab initio* method that computes values using only original physical interpretations and constants of the system, rather than beginning with significant empirical data, thus approximating the wave functions efficiently.[9,10]

The system of interest, the left electrode, scattering region, and right electrode (LSR) system, a model for basic circuitry at the molecular level, needs this method for understanding its eccentricities. Modeling complications exist in this system that hinder a complete analytical solution. These issues mainly come from the non-equilibrium Green's functions along with the aforementioned Kohn-Sham wave-functions, both being the equations that most accurately describe these systems.[6] To resolve such issues, computational methods are used. For example, when designing the tasks in this study the software analyzed, what is depicted in Figure 1 showing the LSR.

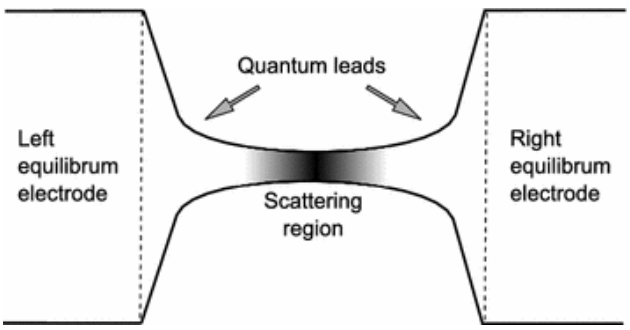

Figure 1: This is a theoretical, graphical rendering of the quantum bridge with electrodes used in calculations to simulate electronics at the quantum level.[11,12]

In such cases software such as SIESTA treats the wiring and electrodes with semi-infinite

behavior, extending the behavior towards infinite atoms while only dealing with the complexity of two atoms.[12] Along with the wire tending infinitely, the electrodes are treated in the same way as the wire.[6] This assumption does not only reduce computation time, but it also reveals other properties not otherwise apparent in discretized systems. Often then generalized behaviors can show somewhat semiconductor-like behavior, lending to behavior similar to a transistor, diode, or new device.[13]

The properties of semiconductors are omnipresent in and ultimately vital for understanding the LSR system. Because quantum effects in electrons are prominent at the nanoscale, behaviors that are normally only seen in macroscopic semiconductors are revealed in conductors as well. This nature can be attributed to the freedom of electrons probabilistically and also the lessened material conduction when only a few atoms are present. Non-classical operations like these can be revealed in the current versus voltage graph (I-V characteristic), and the devices that they behave like are revealed through analyzing the behavior.[14] In particular, it has been noted that non-linear I-V graphs show semiconductor characteristics based on a difference in electron transport mechanisms and such properties can be accentuated in a two-electrode system, as shown in Figure 1.[13] An example of this non-linear I-V that is commonly known would be the transistor as a function of applied voltage which, as shown below, converges to a specific current for the given system.[14]

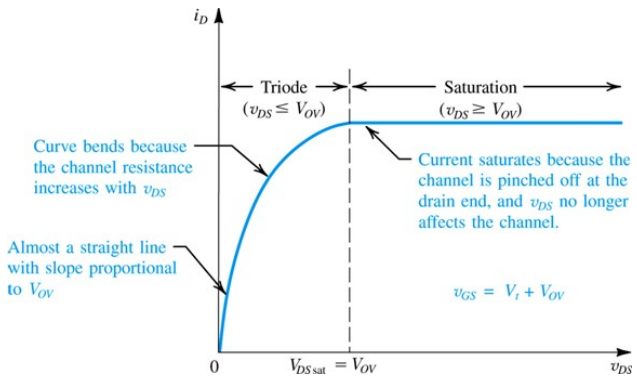

Figure 2: This graphical representation shows the I-V characteristic curve for a transistor. Past a certain voltage, there is nearly constant current, this being called the saturation region.[15]

Since tunneling can be coupled with loose binding, electrons are not held to a surface cohesively, meaning that both properties of insulators and conductors are shown because there is a current that can pass through a device; hence these devices perform as semiconductors.[14]

If these devices act like semiconductors, then their conductive properties will be shown in the measured I-V characteristic. The effectiveness of semiconductor properties can be determined by comparing the measured behavior to well known semiconductors. With this analysis tool, the properties of the LSR studied can be exploited for future use, since the inherent behavior can allow a simply constructed conductor to act as a semiconductor at the quantum level.[16]

In the same way that electrons behave differently to bring out semiconductor behaviors in conductors, the certain discrete states of energy that electrons inhabit also affect the way the current is manifested. In a phenomenon called quantized conductance, electrons can only occupy certain levels of current over a particular range of a potential difference.[17] The conductance is caused by electrons that must move through the electric field induced by the potential difference and that only occupy discrete energies while they transport. Manipulating the definition of current,

$$I = -\frac{dQ}{dt} = -\frac{dQ}{dx}\frac{dx}{dt} = -\lambda v,$$

shows that it can be described as a velocity of charges v moving on a differential length of charge density λ. Since the electrons' velocity is proportional to the potential difference experienced, the measured current exists in quantized states because of electronic energy at the nanoscale.[18] As such, quantized conductance is a phenomenon experienced in the LSR systems described.

While these phenomena have been well-recorded, this study will explore how compositional changes to electrodes in an LSR system affect device behavior. Using computational software, properties about these systems will be determined. While variations in the scatter-

ing region can produce new behavior, an optimal choice of electrode is needed for advanced applications in manufacturing. This exploration will include Li, Be, and Na electrodes with a scattering region that includes a one-dimensional lithium nanowire with an amide functional group attached. This study offers a heightened understanding of the interplay between the electrodes and scattering region under test variations.

Methods and Resources

The use of open source, compilable software that provides an interface with calculations was imperative for accurate modeling of the LSR system. All data acquisition was performed using open source software. The results revealed interesting properties about the LSR variations focused upon.

This study's purpose was to note differences in device operations by comparing results from electrodes of differing compositions. This task required several pieces of software to prepare the particular I-V characteristic that allows insight into generalized device behavior at the nanoscale.

With the goal of isolating effects from electrodes for observation, uniform scattering regions were utilized. The lithium nanowire and the ammonia molecule attached to the wire were constant throughout the entire study. Using these configurations with the electrodes provided an understanding of the differences present based on the electrode's composition.

The study began by using Gabedit, a graphical interface for certain molecular and computational methods.[19] NWChem was used to compute the system's optimized coordinates for configurations in the I-V data calculations.[20] Gabedit generated and ran the input files for the NWChem suite as specified by the drawn geometry. Optimization was performed by a search for convergence in energies in bond lengths using B3LYP as a hybrid functional for DFT.[21,22] The task as 'DFT optimize' provided the necessary lengths of optimized coordinates for the molecules based on their given properties, preparing them for use in involved

calculations of the current and voltage.

Once these optimized coordinates were generated, a spatial conversion program took the angstrom length coordinates to those used by SIESTA and tranSIESTA.[6,12] This can be achieved manually or computationally where a known lattice constant is used to convert these bond lengths and align them with the electrodes in the system allowing for a linear, 1-D flow of electrons.[23] The SIESTA and tranSIESTA jobs could be run with the required conversion of coordinates and preparation of input files.[24] SIESTA then read the files and performed another convergence of coordinates based on *ab initio* principles.

To collect the current information from the system, the voltage was increased with a step size of 0.025 eV. By running the job, sufficient files were created to allow a utility program in the tranSIESTA package called TBTrans to record the actual current for the calibrated system.[25]

The convergence of the system was optimized by running a SIESTA job on the files for each system. The jobs produced a .EIG file containing the eigenvalues of the Kohn-Sham hamiltonian.[24] The TBTrans specifications require this information as a lower and an upper bound for the solving region, and so by inputting these specific values, the knowledge of the system and how it would converge based on the Kohn-Sham wave functions was greatly increased.

To assist in the study, visualizations were prepared using the software XCrysDen.[26] The .XV file used to generate the imaging is created at the beginning of a tranSIESTA job and using a utility that converts this file to a .XSF file, the proper picture can be determined and used to check the system being run and solidifies the tested system.

This provides the process used to construct the I-V characteristics for the LSR with electrode variations. It should be noted that all software and calculations were run in the Linux Ubuntu 16.04 distribution as compatible with the outlined versions of the open-source software used.

This outline is available for the specifics of the study that will be outlined in the Numerical

Results section.

Table 1: This is the summary of all studies conducted on the systems. The system designations are given along with their variations from one another.

Summary of Studied Systems		
System Designation	Electrode Composition	Scattering Region Composition
LELN	Lithium	Lithium Nanowire
LELNA	Lithium	Lithium Nanowire with Amine Group
BELN	Beryllium	Lithium Nanowire
BELNA	Beryllium	Lithium Nanowire with Amine Group
NELN	Sodium	Lithium Nanowire
NELNA	Sodium	Lithium Nanowire with Amine Group

Numerical Results

The basis of the exploration was to find the differing I-V behavior with varied electrodes. The differentiation in results was also made by attaching a device to a scattering region and observing the differences in the I-V characteristic accordingly. These data and figures, graphically presented, detail the results holistically.

Note that each I-V graph details the voltage in 'eV', this is merely meant to denote the voltage with the multiplicative factor of a charge of the electron. Although eV is normally the unit for energy, it is of the same magnitude in this case and is also the way that tranSIESTA requires the voltage to be inputted.

Case of Lithium-Based Electrodes

The two scattering regions studied for the lithium electrodes were a lone lithium nanowire (LELN) and a lithium nanowire with an amine group attached to the two lithium atoms (LELNA).

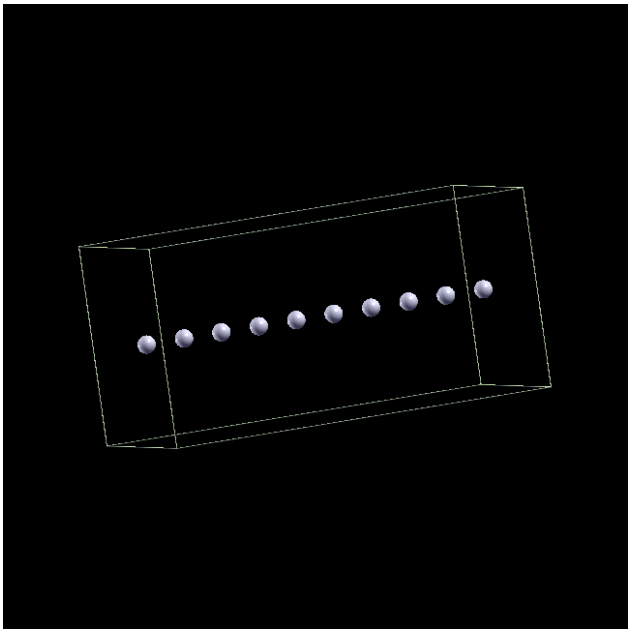

Figure 3: This visualization shows the LELN, two lithium electrodes and the lithium chain.

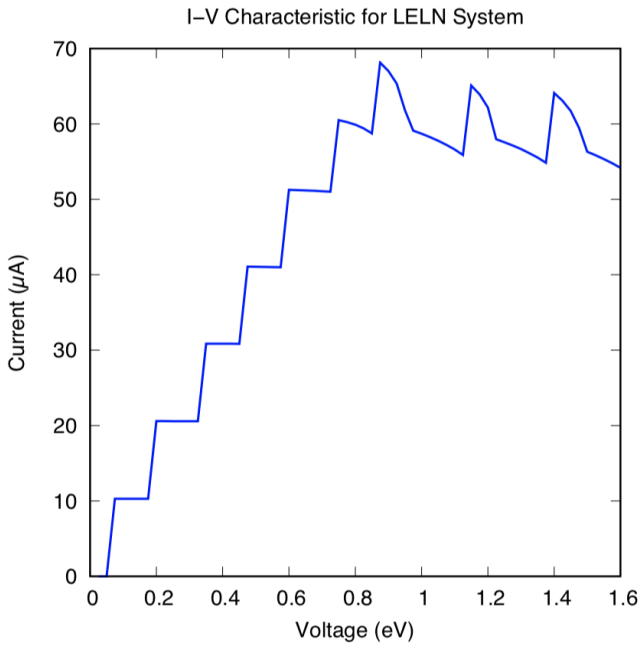

Figure 4: The I-V characteristic for the LELN system as depicted in Figure 3.

Table 2: The optimal conditions for the LELN and LELNA systems as pictured in Figures 3 and 5.

Lattice Constant	Mesh Cutoff
3.0 Å	300.0 Ry

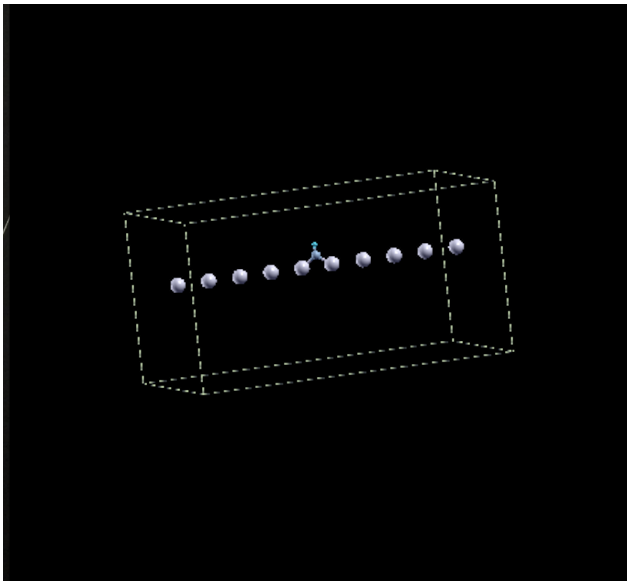

Figure 5: The visualization of the LELNA system, two lithium electrodes and a lithium chain with an amine group attachment.

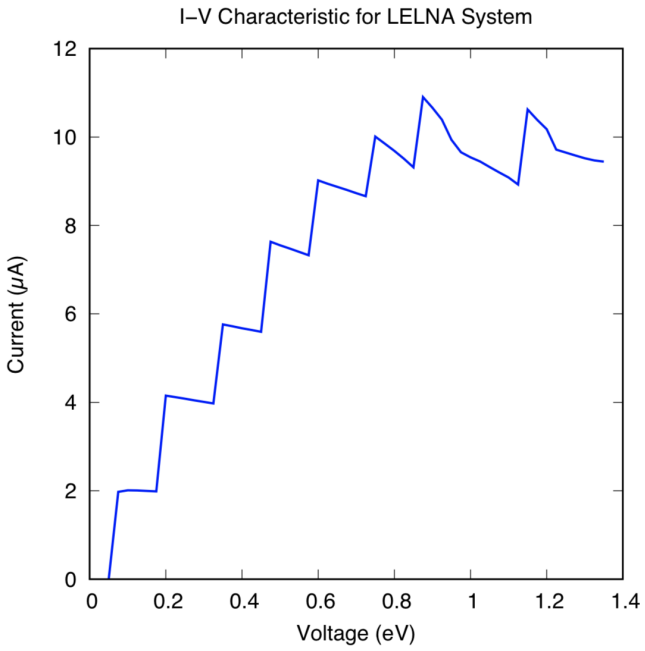

Figure 6: The I-V characteristic for the LELNA system as depicted in Figure 5.

Case of Beryllium-Based Electrodes

The same choices of scattering regions were used in this portion of the study, yet the electrodes were changed to four beryllium atoms in each lead. The two systems considered were a lone lithium nanowire between two electrodes (BELN) and a lithium nanowire with an amine group attachment between the two electrodes (BELNA).

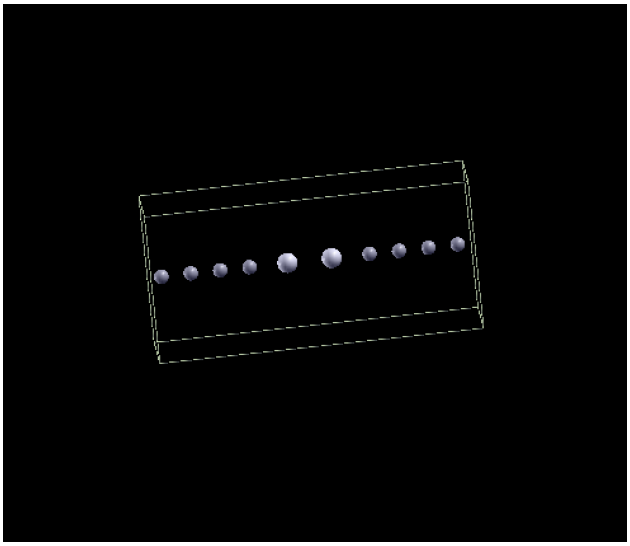

Figure 7: The visualization of the BELN system, two beryllium electrodes and a lithium nanowire.

Table 3: The optimal conditions for the BELN and BELNA systems as pictured in Figures 7 and 9.

Lattice Constant	Mesh Cutoff
2.1 Å	300.0 Ry

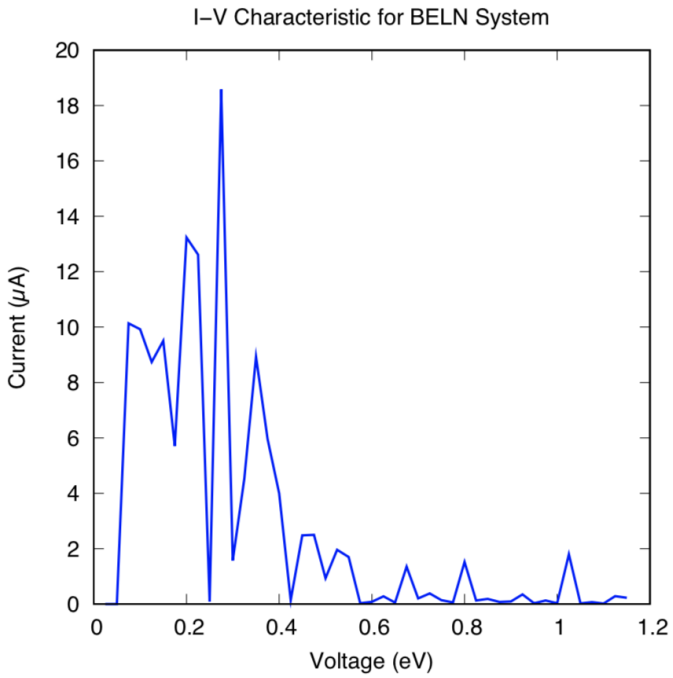

Figure 8: The I-V characteristic for the BELN system, as depicted in Figure 7.

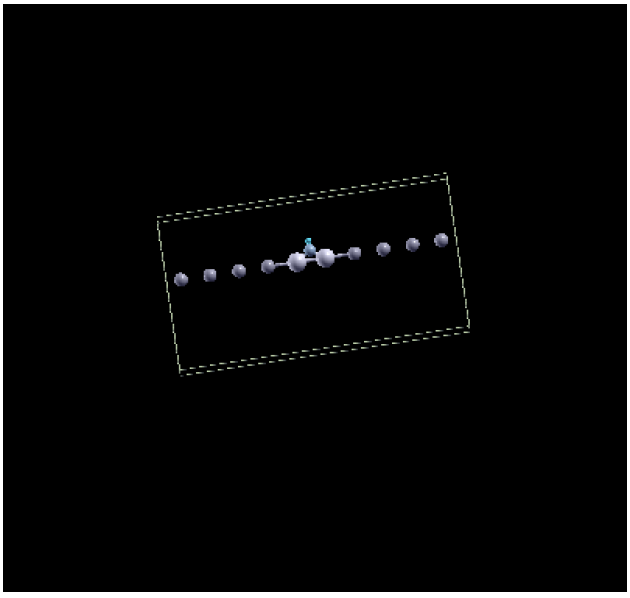

Figure 9: The visualization of the BELNA system, two beryllium electrodes and a lithium chain with an amine group attachment.

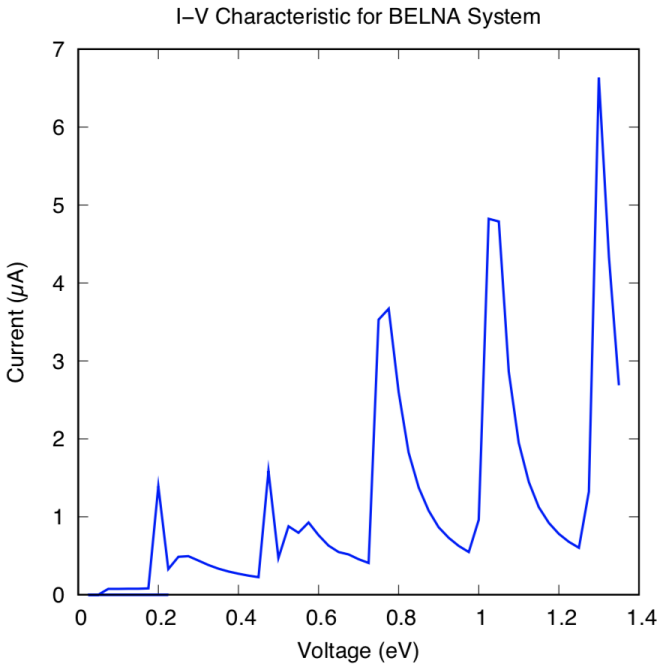

Figure 10: The I-V characteristic for the BELNA system, as depicted in Figure 9.

Case of Sodium-Based Electrodes

The scattering regions remained consistent with the rest of the study. The different electrode composition was from using sodium atoms. This left the systems as the Na electrodes with a lithium nanowire system (NELN) and the Na electrodes with a lithium nanowire and amine group attached.

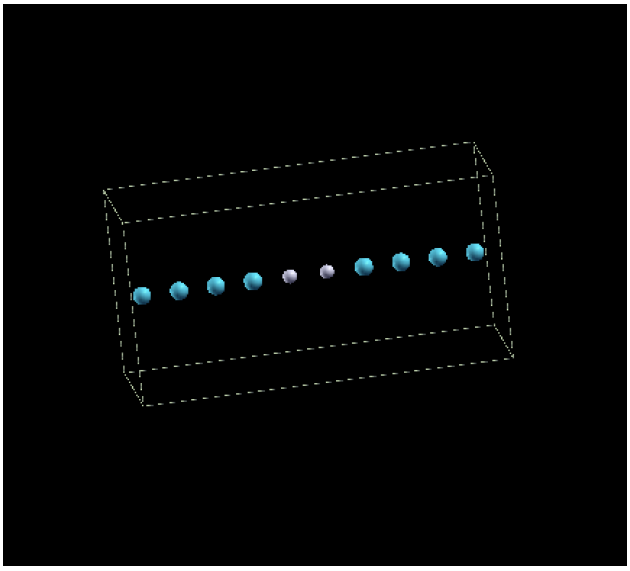

Figure 11: The visualization of the NELN system, two sodium electrodes and a lithium nanowire.

Table 4: The optimal conditions for the NELN and NELNA systems, as pictured in Figures 11 and 13.

Lattice Constant	Mesh Cutoff
3.6 Å	500.0 Ry

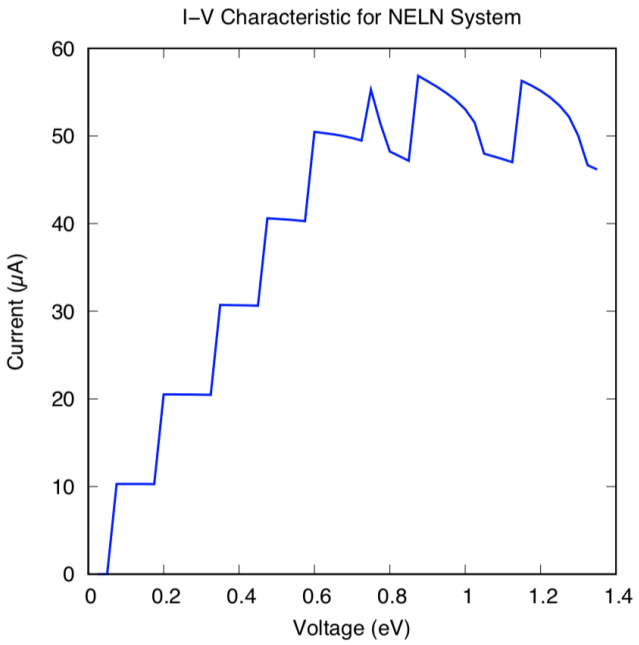

Figure 12: The I-V characteristic for the NELN system, as depicted in Figure 11.

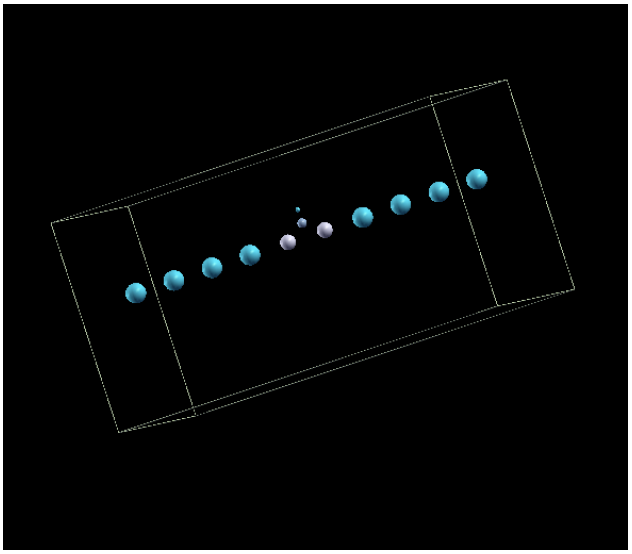

Figure 13: The visualization of the NELNA system, two sodium electrodes and a lithium chain with an amine group attachment.

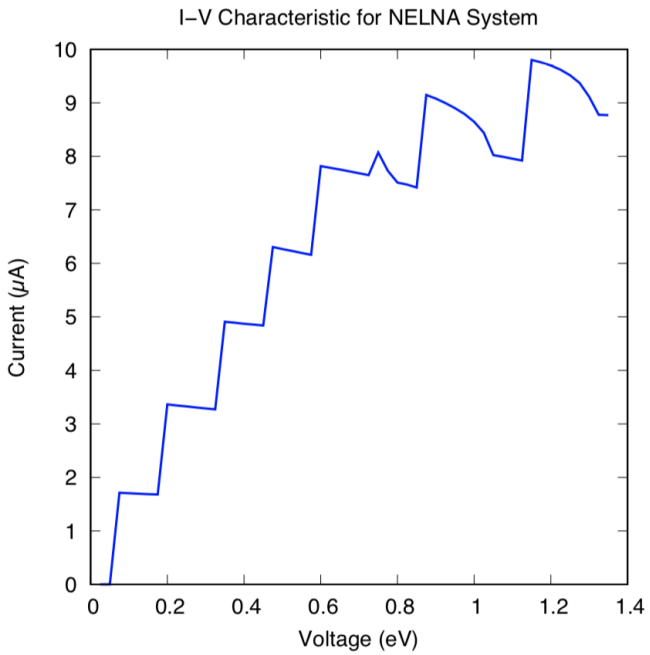

Figure 14: The I-V characteristic for the NELNA system, as depicted in Figure 13.

Analysis of Numerical Results

As aforementioned, the I-V characteristic can give insight about a device's performance. Within the system constraints of the hardware at hand, in all cases a step size of 0.025 eV was used, running the system from 0.0 eV to approximately 1.35 eV. The upper bound was picked due to a generally convergent behavior or predicted trend, but also because computational time at this point exceeded the benefit of gathering data.

Note that in all studies with the amine group attachment that current was measured across the lithium atom and nitrogen atom to show the path difference of electrons in this case. This shows different results than the lithium to lithium bond and can reveal a difference in system orientation and abilities.

The included tables show the optimal lattice constant and mesh cutoff for the systems. The lattice constant controls the scale of the coordinates and their relation in angstroms for a unit in the coordinates of SIESTA, mainly in terms of the lattice vectors one defines for the given system.[12,24] The mesh cutoff is a definition of fineness for the region that SIESTA integrates over, dividing the region for a plane-wave cutoff based on the basis set expansion.[27] A difference of less than 0.1% was adopted for convergence in terms of the lattice constant and mesh cutoff for choice and probing.

At this nano-scale, many of the systems studied acted similarly to semiconductors. This can be characterized by the non-Ohmic behavior of the I-V characteristic. The behavior can be attributed to the way in which electrons are not necessarily bound to a certain path in a metal. Conductors perform at the macroscopic scale because metallic bonding allows valence electrons to be loosely associated to atoms in the material, allowing for charged particles to flow well. Yet with only a few atoms the same behavior is not present, hence, only some behavior of a conductor is allowed, permitting for semiconductor behavior to be revealed.

In particular, the LELN, LELNA, NELN, and NELNA systems conveyed a similar behavior to that is shown in Figure 2, which is the ideal transistor. Although there was not a gate or triode designed for the system, the general sigmoidal curve shape shows that over

increasing voltages the system does reach a saturation region, from the inspected ranges.[15]

With the transistor-like behavior, these four systems showed a stair-stepping behavior. This can be attributed to the quantized energy states of electrons accentuated at the quantum level.[28] This occurrence happens at discrete levels, leading to the stair stepping behavior, as shown in Figures 4, 6, 12 and 14.

The LELN shows the greatest conductance sustained and the NELN shows similar conductance to the LELN, yet a slightly lower saturation current. An explanation for this could come from the difference in the number of electrons that exist in sodium and lithium, creating a different repulsion or field for DFT to create, making a larger system-wide resistance for the sodium electrodes.

The LELNA and NELNA show the same transistor and stepwise behavior, yet have lowered currents, as explained by the alternate path for electrons through the amine group and also through the lithium chain. Another explanation is the polar nature formed through the nitrogen and hydrogen bond. Again, the field method DFT uses to approximate molecular interactions could reduce the number of electrons that flow through the branch of the scattering region. As such, this could explain the lowered conductance in these two cases.

The BELN and BELNA systems showed varied behavior that did not conform to the device standards seen in the other four electrode situations. As seen in both cases, relative maxima are reached in the current measured, though it would fall to a lower point. In the BELNA system the same pattern was sustained in the region viewed, which was a periodically increasing series of maxima and minima. Although not like any device with an analog, this system shows promising and interesting behavior. A periodic nature like in the BELNA could be used for control of currents, assuming a deeper understanding of the peaks and troughs that come with the behavior.

However, a different behavior from the BELNA came with the BELN system. After a global maximum around 0.275 eV, the device gradually falls off to a very low current that represents an 'off' region. Because of the behavior, the BELN acts similarly to some diodes

in how there is a distinct voltage with a maximum current and then a virtual breakdown after this point.

The behaviors of the BELN and BELNA systems show a new device behavior that comes from the beryllium electrodes and the lithium nanowire. The differences in chemical properties can be attributed to the differences between the beryllium electrodes and the lithium/sodium electrodes. In these differences, new device behavior can be attributed to these two systems. The capacities of the beryllium electrodes beckon for a better understanding of how unlike valence electron types bond to create activities in nanoscale devices.

For each system, though, a finer step size and a larger range need to be explored to understand the system fully. These ranges show a sample of the possible behaviors of these small devices and the complications in analysis of the LSR system with varied electrodes.

Conclusions

The six systems studied showed interesting behaviors unlike that of the macroscopic analogs of the LSR system. The Li and Na electrode systems showed similar transistor-like behavior, whereas the beryllium electrode systems conveyed a varied behavior that should be explored more closely with greater computational power. The increasingly periodic nature of the BELNA, with the diode-like BELN shows a different and non-classical operation. The differences in conductivity from the Li and Na systems should be further explored for a best choice of materials in device construction. With these observations, new device behavior has been shown to be omnipresent in simple systems that will soon be implemented ubiquitously in the shrinking electronic world. More studies into this area will yield a greater understanding of the nanoscale electronics that will soon inhabit all aspects of device behavior.

Acknowledgement

The author thanks Professor Gary Washington for his assistance and guidance throughout the duration of the learning and researching process, for without this help none of the preceding work would have been possible. The author also thanks Mr. Bill Epstein and everyone at Pioneer Academics for their aid in logistical matters throughout the project.

References

(1) Geppert, L. Quantum Transistors: Toward Nanoelectronics. 2000.

(2) Simonite, T. *Moore's Law Is Dead: Now What*; 2016.

(3) Taur, Y. *IEEE Spectrum* **1999**, *36*, 25–29.

(4) Trixler, F. *Current Organic Chemistry* **2013**, *17*, 1758–1770.

(5) Sherill, C. D. *Postulates of Quantum Mechanics*; 2000.

(6) Stokbro, K.; Taylor, J.; Brandbyge, M.; Ordejón, P. *Physical Review B* **2002**, *65*.

(7) Delaney, P.; Greer, J. C. *Physical Review Letters* **2004**, *93*.

(8) Sherill, C. D. *An Introduction to Hartree-Fock Molecular Orbital Theory*; 2000.

(9) Sherill, C. D. *Introduction to Density Functional Theory*; 2000.

(10) Friesner, R. A. *Proceedings of the National Academy of Science of the United States of America* **2005**, *102*, 6648–6653.

(11) Ryndyk, D. A. *Theory of Quantum Transport at Nanoscale*; Springer, 2016.

(12) Soler, J. M.; Artacho, E.; Gale, J. D.; García, A.; Junquera, J.; Ordejón, P.; Sánchez-Portal, D. *Journal of Physics: Condesned Matter* **2002**, *14*, 2745–2779.

(13) Wen, J.; Zhang, X.; Gao, H. *Nanotechnology* **2016**, *27*, 1–8.

(14) Feynman, R. *The Feynman Lectures on Physics*; Addison-Wesley, 1964; Vol. 3.

(15) Levkov, S. *Transistor : IV-Characteristic*; 2015.

(16) Fonstad, C. *Introduction to Semiconductors*; 2009.

(17) van Houten, H.; Beenakker, C. *Quantum Point Contacts*; 1996.

(18) Kuemmeth, F.; Bolotin, K. I.; Shi, S.-F.; Ralph, D. C. *Nano Letters* **2008**, *8*, 4506–4512.

(19) Allouche, A. *Journal of Computational Chemistry* **2010**, *32*, 174–182.

(20) Valiev, M.; Bylaska, E. J.; Govind, N.; Kowalski, K.; Straatsma, T. P.; Dam, H. J. V.; Wang, D.; Nieplocha, J.; Apra, E.; Windus, T. L.; de Jong, W. A. *Computer Physics Communications* **2010**, *181*, 1477–1489.

(21) Becke, A. *Journal of Chemical Physics* **1993**, *98*.

(22) Stephens, P.; Devlin, J.; Chabalowski, C.; Frisch, M. *Journal of Chemical Physics* **1994**, *98*.

(23) Washington, G. Coordinate Conversion. Python Script, 2018.

(24) Soler, J. M.; Artacho, E.; Gale, J. D.; García, A.; Junquera, J.; Ordejón, P.; Sánchez-Portal, D.; Martin, R. M. *User's Guide: SIESTA 4.0*; Documentation, 2016.

(25) Falkenberg, J. T.; Brandbyge, M. *Beilstein Journal of Nanotechnology* **2015**, *6*, 1603–1608.

(26) Kokalj, A. *Journal of Molecular Graphics and Modelling* **2000**, *17*, 176–216.

(27) Bylaska, E. J. *Introduction to Plane-Wave Basis Sets and Pseudopotential Theory*.

(28) Griffiths, D. J. *Introduction to Quantum Mechanics*, 2nd ed.; Cambridge University Press, 2017.